

## Understanding the elusive magnetic behavior of manganese clusters

José Mejía-López,<sup>1</sup> Aldo H. Romero,<sup>2</sup> Martín E. García,<sup>3</sup> and J. L. Morán-López<sup>4,\*</sup>

<sup>1</sup>*Facultad de Física, Pontificia Universidad Católica de Chile, Casilla 306, Santiago 22, Chile*

<sup>2</sup>*CINVESTAV Querétaro, Libramiento Norponiente No. 2000, 76230 Querétaro, Mexico*

<sup>3</sup>*Theoretische Physik, Fachbereich Naturwissenschaften, and Center for Interdisciplinary Nanostructure Science and Technology (CINSA-T), Universität Kassel, Heinrich-Plett-Strasse 40, 34132 Kassel, Germany*

<sup>4</sup>*Institute for Computational Engineering and Science, University of Texas at Austin, Austin, Texas 78712-0027, USA*

(Received 8 May 2008; revised manuscript received 24 August 2008; published 6 October 2008)

Manganese is a multifarious element and presents a large variety of behaviors. With the aim of understanding the complex behavior, we performed a systematic study of the magnetic solutions of the manganese dimer as a function of the interatomic distance. The calculation is performed within the framework of an *ab initio* calculation. We show that a remarkable interplay between different magnetic couplings leads to a transition between antiferromagnetic and ferromagnetic couplings as a function of interatomic distance. We present the electronic spectra for the two configurations for different interatomic distances and show clearly the role of the  $4s$  to  $3d$  electron transfer to stabilize the antiferromagnetic solution at short distances. Our results are in good agreement with experiment.

DOI: [10.1103/PhysRevB.78.134405](https://doi.org/10.1103/PhysRevB.78.134405)

PACS number(s): 75.75.+a, 75.50.Tt, 36.40.Cg

### I. INTRODUCTION

The magnetic properties of manganese have represented a challenge for many decades. Manganese is a unique element which exhibits a variety of unusual crystallographic, electronic, and magnetic properties depending on the pressure, temperature, and its environment.<sup>1-8</sup> For instance, the bulk-crystal structure of  $\alpha$ -Mn at ambient conditions is paramagnetic and its crystal structure cell contains 58 atoms. At temperatures below the Néel temperature  $T_N=95$  K, it adopts a complex noncollinear (NC) antiferromagnetic (AFM) phase. In addition, the magnetic phase transition is coupled to a crystal lattice distortion.<sup>9</sup> Upon increasing the temperature to 1000 K, the solid undergoes a crystallographic transition to a cubic lattice with 20 atoms per unit cell.<sup>10</sup> The  $\gamma$  phase is observed in the range from 1368 to 1406 K. Finally, from this last temperature to the melting point  $T_M=1517$ , manganese adopts the  $\delta$  phase, which has a bcc structure.

On the other hand, by quenching the  $\gamma$  phase to room temperature a face-centered-tetragonal structure is stabilized. This phase is antiferromagnetic with a Néel temperature of  $T_N=570$  K. Furthermore, recent high-pressure experiments<sup>11</sup> report a change in phase from the  $\alpha$  to the  $\epsilon$  phase that seems to be an antiferromagnet with bcc structure and Néel temperature of  $T_N=450$  K.

Other interesting characteristic is that dilute solutions of Mn in Cu and Ag behave like spin glasses.<sup>1</sup> These spin-glass systems have the properties of a Heisenberg spin system. However, the presence of anisotropies induces an Ising-type state at small magnetic fields. Other intriguing system with potential technological applications are the mixed-valence manganese oxides known as manganites. They show a variety of magnetic and electronic phenomena such as colossal magnetoresistance (CMR), orbital and charge orderings, etc. Applications of modest external fields may drastically modify the state of such materials, i.e., induce an insulator to metal transition. It has been reported<sup>2</sup> that permanent photo-induced changes in  $\text{Bi}_{0.3}\text{Ca}_{0.7}\text{MnO}_3$  support the feasibility of optical recording in manganites.

Recently, the discovery of complex Mn molecules that function as nanoscale magnets has been reported.<sup>3-5</sup> These intricate molecules with  $\text{Mn}_{12}$  and  $\text{Mn}_4$  complexes act as single-domain magnetic particles that, below their blocking temperature, exhibit magnetization hysteresis. Such single molecule magnets display also resonant tunneling between spin states.<sup>3,4</sup> In both cases the manganese atoms are in the  $\text{Mn}^{3+}$  and  $\text{Mn}^{4+}$  oxidation states with spins  $S=2$  and  $S=3/2$ , respectively. The ions are coupled by a superexchange interaction through oxygen bridges to give a total spin  $S=10$  and  $S=9/2$ .

Consistent with the remarkable properties of Mn compounds mentioned above, experiments show that small manganese clusters exhibit a complex magnetic behavior with signatures of superparamagnetism and magnetic moments  $\mu(n)$  smaller than  $1.5\mu_B/\text{atom}$ .<sup>6,7,12,13</sup> The behavior of  $\mu(n)$  as a function of  $n$  is strongly nonmonotonous.<sup>12,13</sup> In a recent publication we have addressed this problem and offered a possible explanation on the context of noncollinear solutions for the magnetic-moment arrangements.<sup>14</sup>

Finally, the most simple manganese molecule, the dimer is not fully understood. From the experimental point of view, the bond length obtained by electron spin resonance spectroscopy is  $3.4 \text{ \AA}$ , which is very large as compared with the bulk value  $d_0=2.89 \text{ \AA}$ . The measurements were performed by depositing the dimer in rare-gas matrices and found that the dimer has a very low dissociation energy  $D_0=0.1 \text{ eV}$ , and the atomic spins couple antiferromagnetically.<sup>7</sup> A resonance Raman experiment also supports the singlet antiferromagnetic ground state<sup>15</sup> ( $^1\Sigma_g^+$ ). For an extensive review on the experimental research on transition metal and lanthanide small clusters, Lombardi and Davis<sup>8</sup> can be consulted.

It is clear that in an attempt to disentangle the complex behavior of manganese one must try to understand the properties of the dimer as a basic unit. Understanding the magnetic coupling of two manganese atoms as a function of distance, and as first approximation, it may shed some light on what to expect in more complex systems if one knows the

distance between them. In recent years, this subject has been a field of intensive theoretical and experimental research but up to now no consensus on its properties has been achieved.

One of the earliest calculations on  $\text{Mn}_2$ ,<sup>16</sup> based on the Hartree-Fock approximation, obtained an antiferromagnetic ground state with a bond length of 2.88 Å. More recently, different theoretical determinations of the magnetic and electronic structure of  $\text{Mn}_2$  have been reported within the framework of the density-functional theory<sup>17–19</sup> and molecular-orbit methods.<sup>20–22</sup> The density-functional theory calculations yield a ferromagnetic (FM) ground-state solution, but the antiferromagnetic solution differs only slightly in energy. Furthermore, a careful analysis within an all-electron scheme came to the conclusion that  $\text{Mn}_2$  exhibit multiple magnetic and structural minima.<sup>17</sup> On the other hand, the MO calculations by Wang and Chen<sup>21</sup> and Yamamoto *et al.*<sup>22</sup> yield an antiferromagnetic ground state.

The experimental evidence and the theoretical works mentioned above suggest that the most probable scenario for the magnetic properties of the dimer and small Mn clusters is that of almost degenerate different spin configurations. Therefore, the correct approach to describe their magnetic structure must include noncollinearity. The importance of this property was recognized recently by a calculation which yields a noncollinear magnetic configuration for  $\text{Mn}_6$ .<sup>23</sup>

Moreover, the fact that the ferromagnetic and antiferromagnetic solutions are very close in energy, in particular, for very small clusters<sup>18</sup> could also lead to spin frustration in larger clusters. As mentioned above, the overall size dependence of  $\mu(n)$  measured by Knickelbein<sup>12,13</sup> was theoretically described recently<sup>14</sup> on the basis of a noncollinear model for the magnetic moments ground-state orientations.

In this paper, we extend the theoretical description of the dependence of the electronic and magnetic solutions on the interatomic distance for  $\text{Mn}_2$ . We find that the magnetic coupling depends very sensitively on the interatomic distance. For short distances the ground state is antiferromagnetic but it changes to ferromagnetic at  $d=3.06$  Å. In particular in our calculation the ground state is antiferromagnetic with an interatomic distance  $d=2.89$  Å.

The rest of the paper is organized as follows. In Sec. II we give the details of the calculation. The results and their discussion are contained in Sec. III. Our conclusions are presented in Sec. IV.

## II. CALCULATION

We performed collinear and noncollinear *ab initio* determination of the magnetic properties of  $\text{Mn}_2$ . Our results sug-

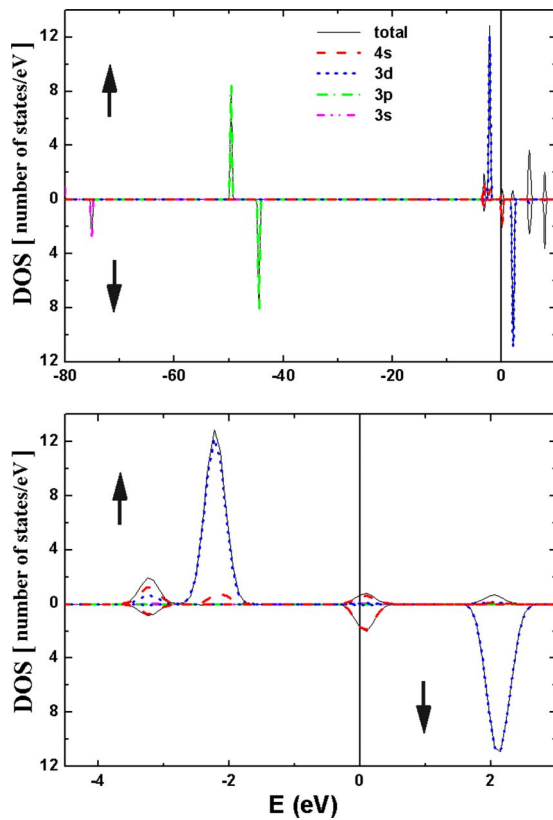


FIG. 1. (Color online) Spin resolved density of states (DOS) of  $\text{Mn}_2$  in the AFM state for an interatomic distance of  $d=2.6$  Å. The upper figure corresponds to contributions from the  $s$  and  $d$  orbitals of the whole dimer. Bottom figure: close up of the spin resolved DOS in the AFM state for a small energy window around the HOMO. The  $y$  units are states per eV.

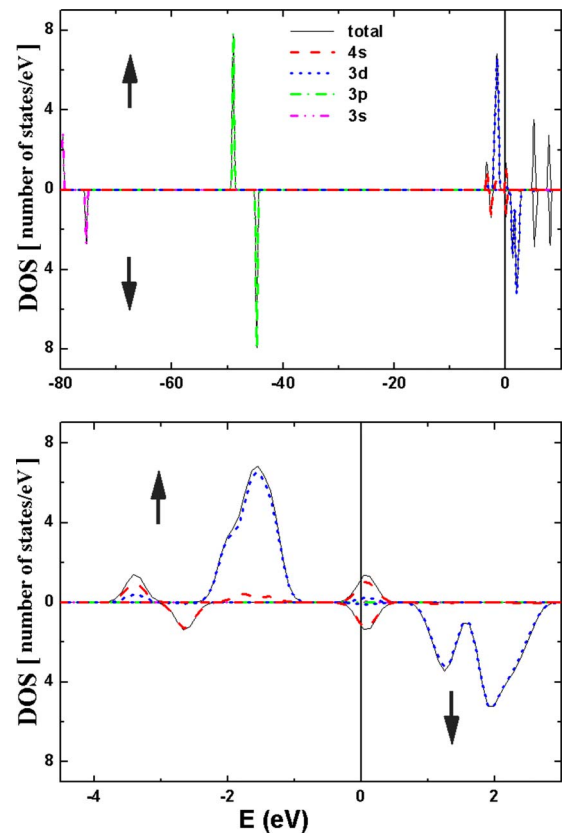


FIG. 2. (Color online) Spin resolved DOS of  $\text{Mn}_2$  in the FM state for an interatomic distance of  $d=2.6$  Å. The upper figure corresponds to contributions from the  $s$  and  $d$  orbitals of the whole dimer. Bottom figure: close up of the spin resolved DOS in the AF state for a small energy window around the HOMO. The  $y$  units are states per eV.

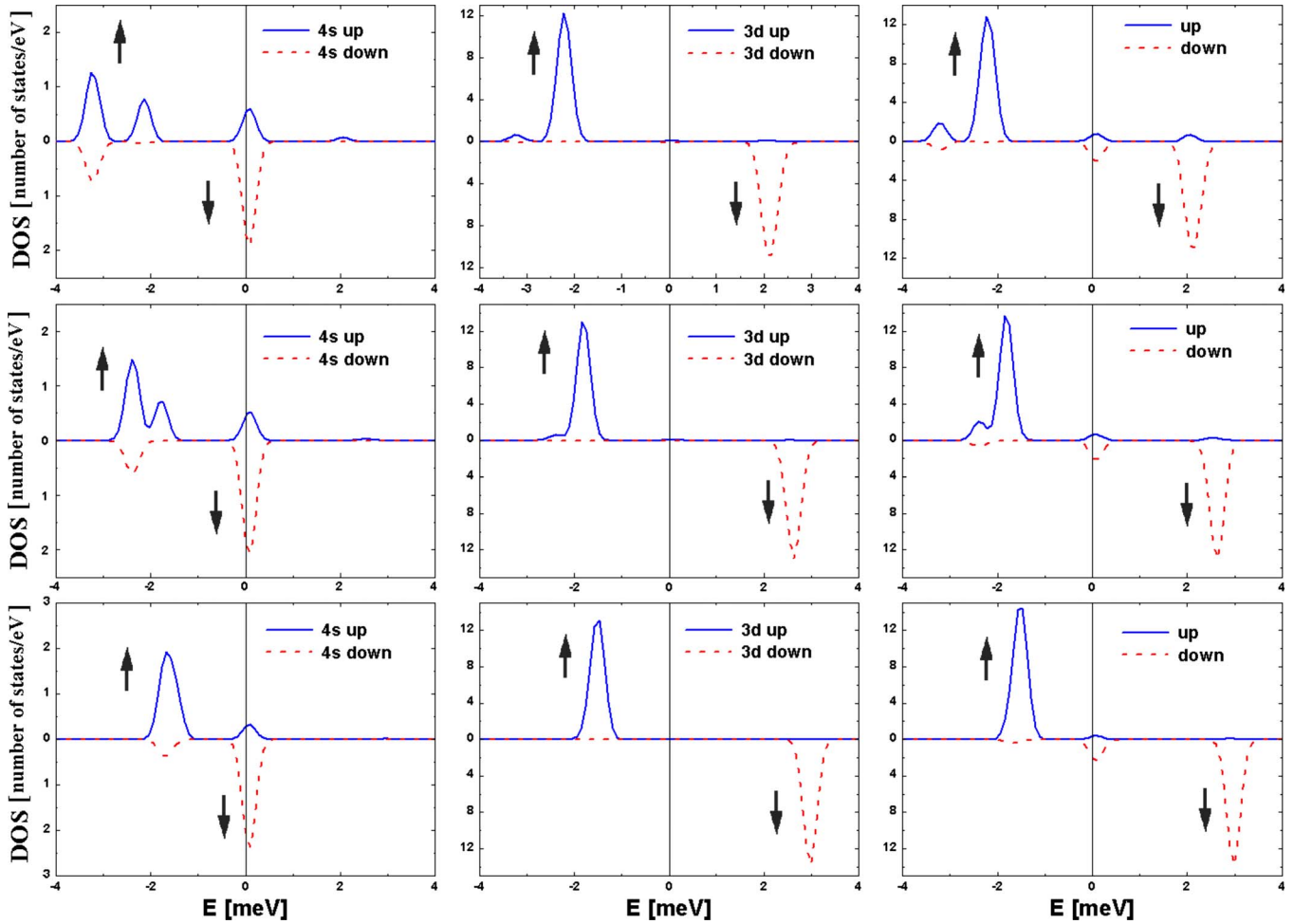


FIG. 3. (Color online) Spin resolved DOS of  $Mn_2$  in the AFM state for different interatomic distances:  $d=2.6 \text{ \AA}$  (top panel),  $d=3.06 \text{ \AA}$  (middle panel), and  $d=3.6 \text{ \AA}$  (bottom panel). Left and middle figures correspond to contributions from the  $s$  and  $d$  orbitals from both atoms, while right figures correspond to total contribution of  $s$ ,  $p$ , and  $d$  orbitals coming from each one of the atoms. The  $y$  units are states per eV.

gest that a remarkable competition between kinetic and exchange-correlation energies leads to almost degenerate spin configurations. To determine the electronic and magnetic properties of the dimer we have used the SIESTA code,<sup>24</sup> which performs a fully self-consistent density-functional calculation to solve the Kohn-Sham equations in a localized basis set. We included spin polarization, both collinear and noncollinear,<sup>25</sup> in the local-density approximation (LDA). The ionic pseudopotentials<sup>26</sup> were generated from the atomic configurations  $[Ne]3s^23p^63d^54s^2$ , core radii of 1.50, 1.50, 1.30, and 2.20 a.u. for the  $s$ ,  $p$ ,  $d$ , and  $f$  components, respectively, and a core correction of 0.7 u.a. The basis set used for the present work to describe the valence states is a double- $\zeta$  set with a confining energy shift of 50 meV. We tested the energy convergence to choose the most appropriate energy shift. We did also performed some other calculations to prove the reliability of our results with respect to the basis set, as performed in Ref. 14.

We calculated the minimal energy solution of the Kohn-Sham equations by fixing the dimer distance and by assuming a given magnetic configuration (ferromagnetic and antiferromagnetic). We should also point out that in or-

der to check the validity of our conclusions, we performed similar collinear calculations with two other exchange correlations.<sup>27,28</sup> We obtained that the minimal Mn dimer distance is different (3.18 and 3.34  $\text{\AA}$ , respectively), but the transition from AFM to FM state is produced by the same physical effects that we explain below. Furthermore, we also performed the calculation by allowing that the magnetic moments of each atom take any arbitrary direction and adopt the direction of minimal energy, i.e., noncollinearity. All calculations were performed with an energy convergence better than 0.1 meV.

As mentioned below, we studied the charge transfer. In particular we calculated this quantity from the change in the Mulliken population per atom as function of distance. This analysis allow us to deduce the change in the electronic charge on the various orbitals in each manganese atom.

### III. RESULTS AND DISCUSSION

We present in Fig. 1 the spin resolved electronic occupation spectra obtained assuming an AFM arrangement for an interatomic distance  $d=2.6 \text{ \AA}$ . Here, we have added a small

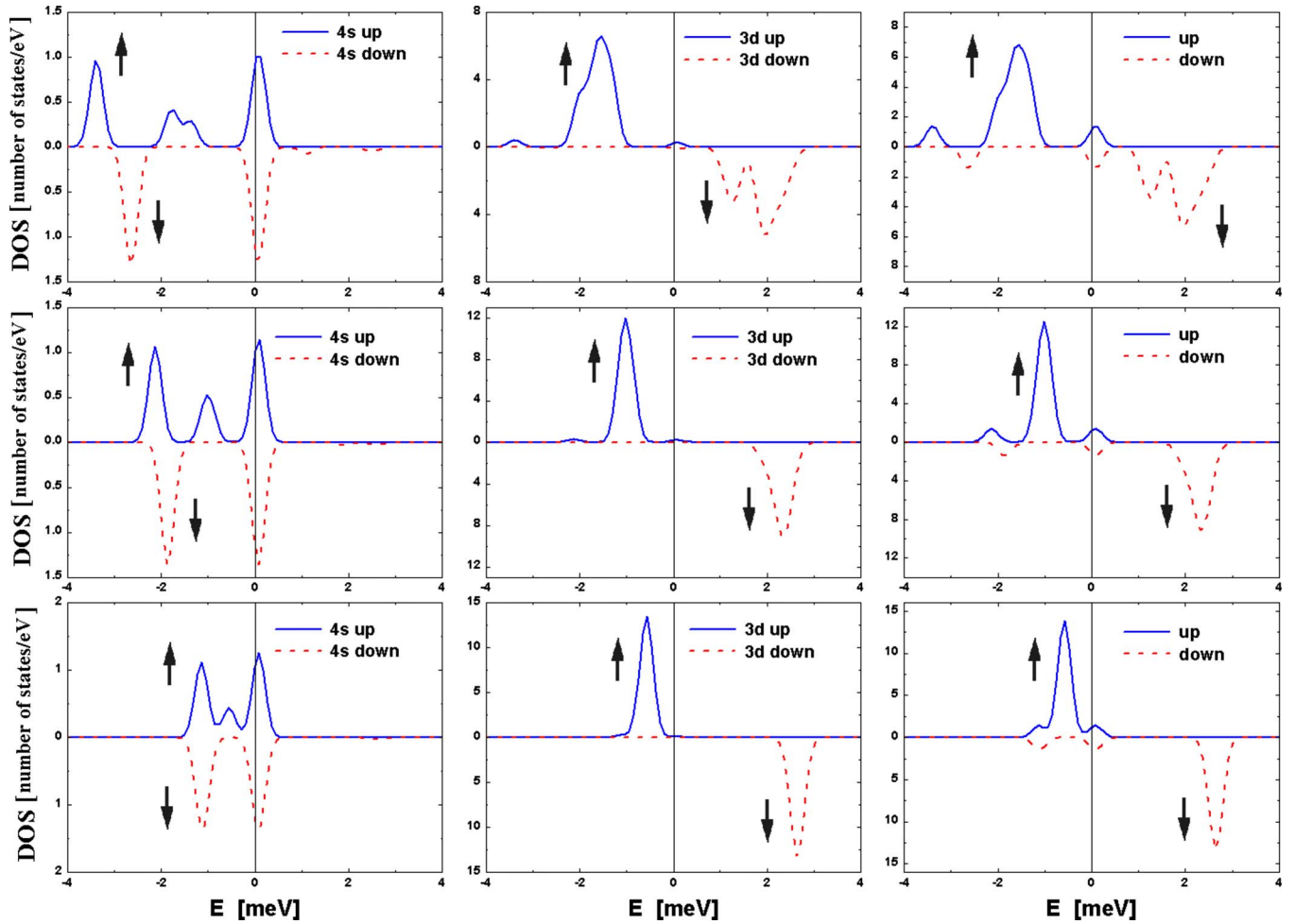


FIG. 4. (Color online) Spin-resolved DOS of  $\text{Mn}_2$  in the FM state for different interatomic distances:  $d=2.6 \text{ \AA}$  (top panel),  $d=3.06 \text{ \AA}$  (middle panel), and  $d=3.6 \text{ \AA}$  (bottom panel). Left and middle figures correspond to contributions from the  $s$  and  $d$  orbitals from both atoms, while right figures correspond to total contribution of  $s$ ,  $p$ , and  $d$  orbitals coming from each one of the atoms. The  $y$  units are states per eV.

imaginary part around the energy levels to wide them up and the zero of energy is taken at the highest occupied molecular-orbital (HOMO) energy level. The contributions coming from the different electronic levels are shown. One notices that the  $3s$  and  $3p$  electronic states are fully occupied since they lie deep in energy and do not contribute to the magnetic moment. The lower part contains a close up to the region around the zero of energy. As shown here, the electrons near the HOMO are the  $4s$  and  $3d$  electrons. The small peaks correspond to the  $4s$  electrons. There is a small number of  $s$  states with spin up above the HOMO. As discussed below, these states bring a decrease in the total magnetic moment  $\mu$ .

In Fig. 2 we show the results for the spin-resolved electronic occupation spectra assuming the same interatomic distance but for the ferromagnetic arrangement. As expected, the role of  $3s$  and  $3p$  electrons is also irrelevant for the magnetic properties of this state of the dimer. In the lower panel we present a close up to the region around the HOMO. In this case the number of spin-up  $d$  electrons is 5 and the one of spin-down electrons is zero. In the case of the  $4s$  orbitals, there is one electron with spin up and other with spin down.

The evolution of the electronic occupations as a function of the interatomic distance for the antiferromagnetic state is shown in Fig. 3. The panels correspond to  $d=2.6$ ,  $3.06$ , and  $3.6 \text{ \AA}$ , respectively. One sees clearly how the  $s$  orbitals reduce their splitting and the  $s$ -states above the HOMO practically disappear at  $d=3.6 \text{ \AA}$ .

A different situation is obtained when the magnetic arrangement is FM. The results for the electronic occupation for the three interatomic distances are plotted in Fig. 4. In this case, as the distance between atoms increase, the spin-down  $d$ -electronic state is the only one above the HOMO and is therefore empty. This yields a magnetic moment  $\mu=5\mu_B$ .

In Fig. 5 we plot how the charge on the  $4s$  and  $3d$  levels change as a function of distance for the antiferromagnetic state. As the distance is decreased, the  $3d$  down electron state increases its charge at the expenses of the spin-down level. Due to hybridization there is a small charge transfer between  $s$  and  $d$  states. If the distance is too short the  $4s$  up electrons may be transferred in a larger amount than the spin down. As discussed below, this brings a negative contribution to the total magnetic moment. Let us recall that the results are

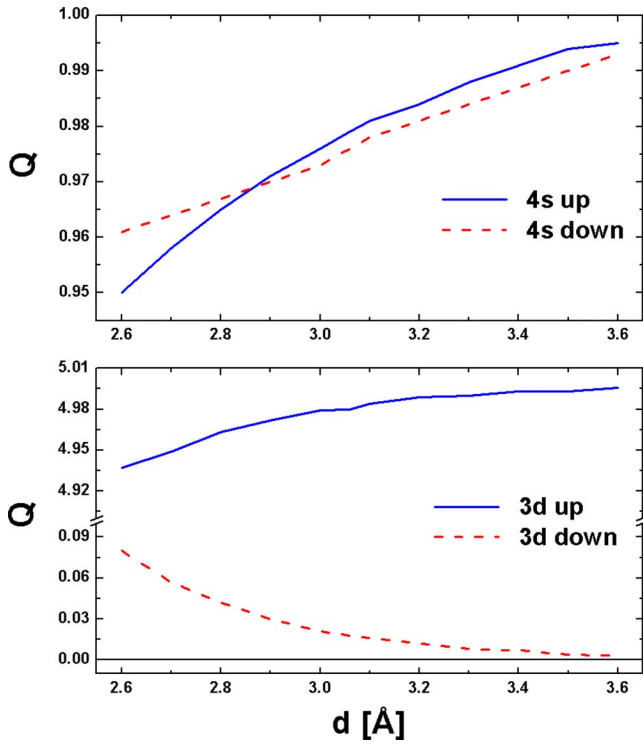


FIG. 5. (Color online) Charge  $Q$  of the  $4s$  and  $3d$  orbitals of  $Mn_2$  in the AF state as a function of the interatomic distance.

given per atom and the  $3s$  and  $3p$  electrons are not taken into account in this sum.

The dependence of the occupation of the  $4s$  (upper panel) and  $3d$  (middle panel) levels on the distance between nuclei

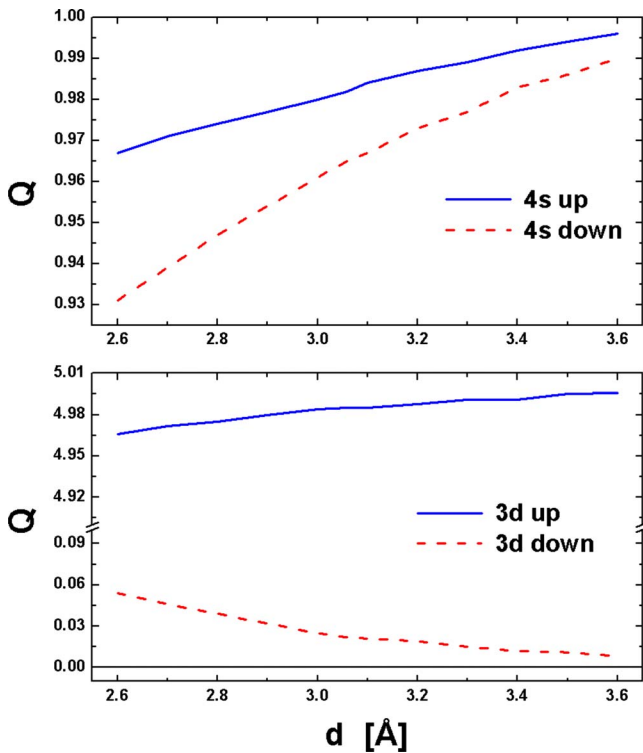


FIG. 6. (Color online) Charge  $Q$  of the  $4s$  and  $3d$  orbitals of  $Mn_2$  in the FM state as a function of the interatomic distance.

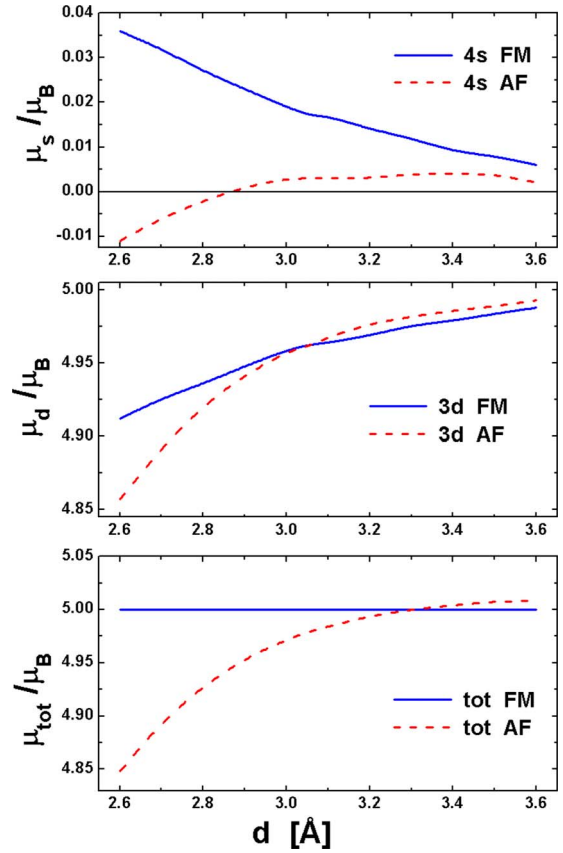


FIG. 7. (Color online) Magnetic moment for each of the atoms of  $Mn_2$  as a function of dimer distance.

for the ferromagnetic alignment is given in Fig. 6. The occupation of up  $3d$  electrons is close to 5 and the increase in down electrons as the distance decreases comes more from  $4s$  electrons. It is also to be noticed that there is no crossover

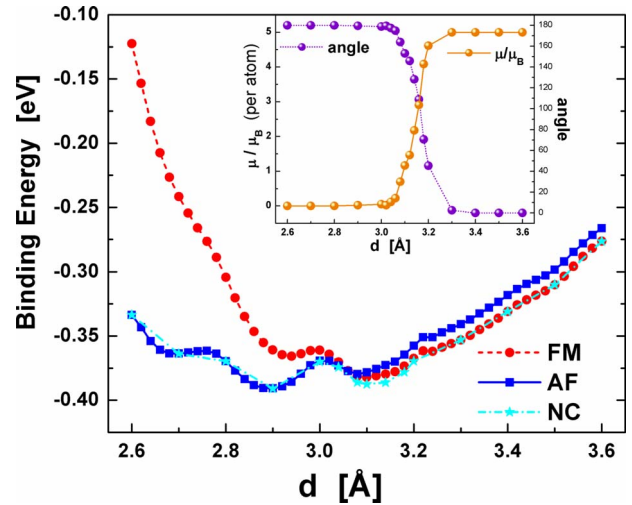


FIG. 8. (Color online) Total energy for  $Mn_2$  as a function of dimer distance for the ferromagnetic, antiferromagnetic, and non-collinear solutions. In the Inset we show the relative orientation between the magnetic moments in the dimer (non collinear) and the change in average magnitude of the magnetic moment as a function of the interatomic distance.

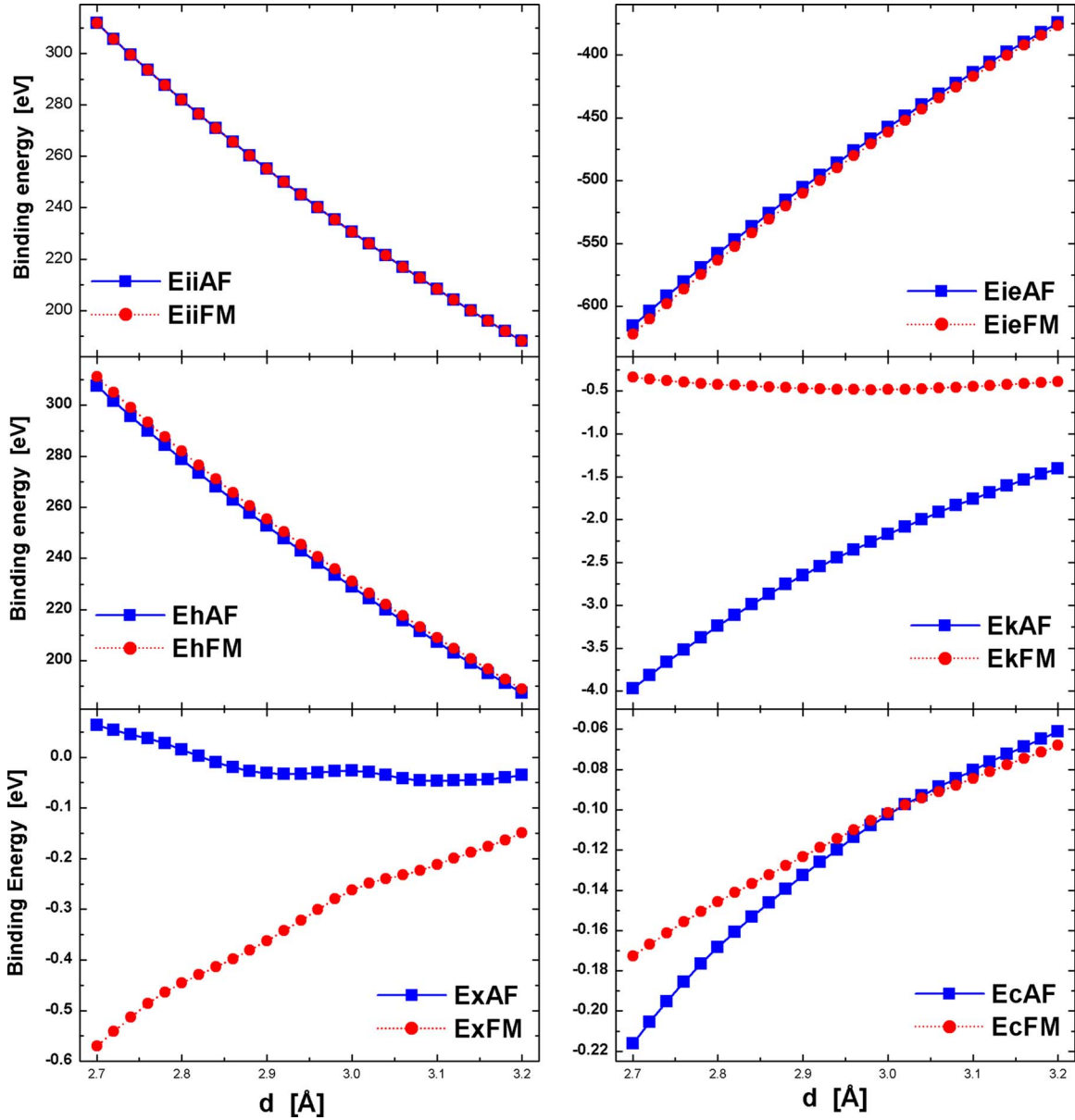


FIG. 9. (Color online) Contributions to the total binding energy as a function of dimer length. The three panels on the right-hand side are the contributions arising from ion-ion, Hartree, and exchange contributions, respectively. On the left three panel we show those arising from ion-electron, kinetic, and correlation contributions, respectively.

behavior in the distance dependence of the charge of up and down electrons. This behavior brings a positive contribution to the total magnetic moment.

We show in Fig. 7 the magnetic moments generated by  $4s$  and  $3d$  electrons. The magnetic moment produced by  $d$  electrons is smaller in the AFM than the FM case for short distances, and both become equal at a distance of about 3.06 Å. Above that value the FM arrangement has a magnetic moment smaller but very similar value to the AFM solution. A more interesting behavior is observed in the  $s$  magnetic moment, which is negative for the AFM state at small values of the interatomic distance. In contrast, the magnetic moment of the ferromagnetic arrangement increases monotonously as the interatomic distance gets shorter. The lower panel contains the distance dependence of the total magnetic moment on the two cases (FM and AFM).

In most of the *ab initio* calculations on Mn clusters reported previous to this work a ferromagnetic ground state for  $Mn_2$ , and a change from ferromagnetic to antiferromagnetic behavior for increasing number of manganese atoms in the cluster was obtained.<sup>17–19</sup> The antiferromagnetic behavior was first obtained for clusters with five<sup>18</sup> and nine atoms.<sup>17</sup> Although in a more recent calculation<sup>23</sup> the appearance of noncollinear solutions were obtained for  $Mn_6$ .

In contrast, our calculations yield an antiferromagnetic ground state with a bond length of  $d_0=2.890$  Å. This result for the magnetic ordering of the dimer is in agreement with the experimental evidences mentioned in Sec. I.<sup>7,8</sup> However, it must be pointed out that the ferromagnetic, antiferromagnetic, and noncollinear states are almost degenerate. We show in Fig. 8 the distance dependence of the total energy for the FM, AFM, and NC solutions. There is a remarkable

distance dependence exhibited by the magnetic coupling, going from AFM to a NC arrangement to FM as the interatomic distance increases. The most important feature of Fig. 8 is that there is a crossing between the FM and AFM curves at  $d_c=3.06$  Å, which determines the interatomic distance at which the ground-state changes from AFM to FM. This crossing between the two different magnetic states is also present in singly charged manganese dimers (with charges of +1.0 and -1.0). Note also that the equilibrium distances (2.8 Å for  $Mn_2^+$  and 2.6 Å for  $Mn_2^-$ ) are smaller than in the neutral dimer.

It is important to note that the energy of the noncollinear solution coincides with the AFM curve for distances  $d < d_c$  and with the FM curve for  $d > d_c$ . This means that the dimer shows collinear magnetism for almost all distances. However, we obtain an interesting behavior around  $d=d_c$ , where the noncollinear solution has a slightly lower energy than the collinear curves. This is due to the fact that at this point the AFM and FM states have the same energy and therefore an intermediate noncollinear state leads to an energy decrease.

Another important feature shown by Fig. 8 is the appearance of multiple minima in the three energy curves. It is important to note that the depths of all energy minima are larger than the error  $\Delta\epsilon$  of the energy calculations.  $\Delta\epsilon < 1$  meV, whereas the heights of the energy barriers are at least 5 meV. It is possible that inclusion of van der Waals interactions (which are not taken into account by the LDA) might lead different and more pronounced minimum. In the inset we show the relative orientation between the magnetic moments in the noncollinear dimer as well as the change in average magnitude of the magnetic moment as a function of dimer length.

The various minima of the energy are produced by the competition of the various interactions. The different energy terms (exchange, correlation, kinetic energy, Hartree energy, and core-core repulsion) compensate each other in such a way that small variations in magnitude of these terms lead to shifts, amplification, or disappearance of some of the minima, as it is shown in Fig. 9, where we show that the competition between kinetic energy and the exchange correlation is responsible for the variations in the potential-energy surface.

We have analyzed the distance dependence of the different terms contributing to the cohesive energy of the dimer (see Fig. 9). It turns out that most of the energy terms cancel each other, except the correlation energy, which plays then the fundamental role. Since the FM and the AFM configurations of the dimer are very close in energy, and due to the change in magnetic character for increasing distances, one should not expect a clear magnetic ordering in small clusters, but rather a competition between both types in larger clusters where manganese atoms may be located at distances that favor FM or AFM coupling. The fact that nearest neighbors will tend to order antiferromagnetically, whereas further neighbors will favor a ferromagnetic ordering leads to non-collinear effects and domain formation in order to avoid spin frustration as much as possible.

The behavior shown in Fig. 8 can be interpreted as follows. For short interatomic distances the strong overlap of 3d-orbitals and hybridization effects with 4s electrons lead to

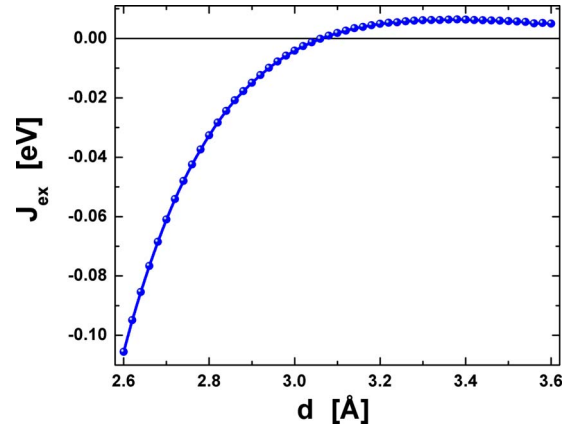


FIG. 10. (Color online) Exchange coupling for  $Mn_2$  as a function of dimer distance.

electron delocalization, which favors antiferromagnetism. In contrast, for long distances, localization becomes more important and the low hybridization with 4s states lead to a ferromagnetic ground state.

One can analyze the crossing of energy curves within the framework of magnetic coupling constants. We have determined an effective exchange coupling constant  $J(d)$  between localized spins at the Mn atoms as defined by

$$J(d) = [E(d)^{\uparrow\downarrow} - E(d)^{\uparrow\uparrow}] / 2 \quad (1)$$

as a function of the interatomic distance  $d$ . This behavior is shown in Fig. 10. As expected, we obtain  $J > 0$  for  $d < d_c$  (antiferromagnetic coupling) and  $J < 0$  for  $d > d_c$  (ferromagnetic coupling).

#### IV. CONCLUSIONS

We have performed a theoretical description of the dependence of the electronic and magnetic solution on the interatomic distance for  $Mn_2$ . We analyzed in detail the electronic occupation of the 4s and 3d states and stressed the differences between the FM and AFM states. We find that the magnetic coupling depends very sensitively on the interatomic distance. For short distances the ground state is antiferromagnetic but it changes to ferromagnetic at  $d=3.06$  Å. In particular in our calculation the ground state is antiferromagnetic with an interatomic distance  $d=2.89$  Å.

The calculation was performed by assuming collinear, ferromagnetic, and antiferromagnetic, and noncollinear arrangement between spins within the framework of the *ab initio* SIESTA code.<sup>24</sup> The basis set used for the present work to describe the valence states is a double- $\zeta$  set with a confining energy shift of 50 meV.

Our results suggest that a remarkable competition between kinetic and exchange-correlation energies leads to almost degenerate spin configurations. We obtain that the correlation energy favors antiferromagnetic behavior for short distances, while for larger atomic separations, the correlation energy of the ferromagnetic state makes it the most stable. Due to this effect, one should not expect a clear unique magnetic ordering in small clusters. The scenario gets more com-

plicated in larger clusters where manganese atoms may be located at distances that favor FM or AFM coupling. This competition may be the reason for the complex behavior of manganese. Furthermore, the fact that nearest neighbors will tend to order antiferromagnetically, whereas further neighbors will favor a ferromagnetic ordering leads to noncollinear effects and domain formation to overcome spin frustration as much as possible.

#### ACKNOWLEDGMENTS

J.M.-L. acknowledges support FONDECYT under Grants No. 1050066 and No. 7050111, and from the Millennium

Sciences Nucleus “Condensed Matter Physics” Grant No. P02-054F. A.H.R. was supported by Project No. J-59853-F from CONACYT-Mexico. M.E.G. acknowledges the kind hospitality at the IPICYT and also support from the DFG through Grant No. SPP1153. J.L.M.-L. acknowledges the support of the J. Tinsley Oden Faculty Fellowship Research Program in the Institute for Computational Engineering and Sciences at The University of Texas at Austin and the partial support by CONACYT under Grant No. 61417 S-3131. The use of computer resources from the Centro Nacional de Supercomputo (CNS) of the Instituto Potosino de Investigación Científica y Tecnológica (IPICYT), SLP, México, is also acknowledged. Useful discussions with P. Schlottmann are kindly acknowledged.

\*On sabbatical leave from Instituto Potosino de Investigación Científica y Tecnológica.

- <sup>1</sup>D. Chu, G. G. Kenning, and R. Orbach, *Phys. Rev. Lett.* **72**, 3270 (1994).
- <sup>2</sup>I. I. Smolyaninov, V. N. Smolyaninova, C. C. Davis, B. G. Kim, S. W. Cheong, and R. L. Greene, *Phys. Rev. Lett.* **87**, 127204 (2001).
- <sup>3</sup>J. R. Friedman, M. P. Sarachik, J. Tejada, and R. Ziolo, *Phys. Rev. Lett.* **76**, 3830 (1996).
- <sup>4</sup>W. Wernsdorfer, N. Aliaga-Alcalde, D. N. Hendrickson, and G. Christou, *Nature (London)* **416**, 406 (2002).
- <sup>5</sup>R. Sessoli, D. Gatteschi, A. Caneschi, and M. A. Novak, *Nature (London)* **365**, 141 (1993).
- <sup>6</sup>K. M. Mertes, Y. Suzuki, M. P. Sarachik, Y. Myasoedov, H. Shtrikman, E. Zeldov, E. M. Rumberger, D. N. Hendrickson, and G. Christou, *Solid State Commun.* **127**, 131 (2003).
- <sup>7</sup>C. A. Baumann, R. J. Van Zee, S. V. Bhat, and W. Weltner, Jr., *J. Chem. Phys.* **78**, 190 (1983).
- <sup>8</sup>J. R. Lombardi and B. Davids, *Chem. Rev. (Washington, D.C.)* **102**, 2431 (2002).
- <sup>9</sup>D. Hobbs, J. Hafner, and D. Spišák, *Phys. Rev. B* **68**, 014407 (2003).
- <sup>10</sup>J. Hafner and D. Hobbs, *Phys. Rev. B* **68**, 014408 (2003).
- <sup>11</sup>H. Fujihisa and K. Takemura, *Phys. Rev. B* **52**, 13257 (1995).
- <sup>12</sup>M. B. Knickelbein, *Phys. Rev. Lett.* **86**, 5255 (2001).
- <sup>13</sup>M. B. Knickelbein, *Phys. Rev. B* **70**, 014424 (2004).
- <sup>14</sup>J. Mejía-López, A. H. Romero, M. E. Garcia, and J. L. Morán-López, *Phys. Rev. B* **74**, 140405(R) (2006).
- <sup>15</sup>K. D. Bier, T. L. Haslett, A. D. Kirkwood, and M. Moskovits, *J. Chem. Phys.* **89**, 6 (1988).
- <sup>16</sup>R. K. Nesbet, *Phys. Rev.* **135**, A460 (1964).
- <sup>17</sup>M. R. Pederson, F. Reuse, and S. N. Khanna, *Phys. Rev. B* **58**, 5632 (1998).
- <sup>18</sup>P. Bobadova-Parvanova, K. A. Jackson, S. Srinivas, and M. Horoi, *Phys. Rev. A* **67**, 061202(R) (2003); *J. Chem. Phys.* **122**, 014310 (2005).
- <sup>19</sup>J. Harris and R. O. Jones, *J. Chem. Phys.* **70**, 830 (1979).
- <sup>20</sup>C. W. Bauschlicher, Jr., *Chem. Phys. Lett.* **156**, 95 (1989).
- <sup>21</sup>B. Wang and Z. Chen, *Chem. Phys. Lett.* **387**, 395 (2004).
- <sup>22</sup>S. Yamamoto, H. Tatewaki, H. Moriyama, and H. Nakano, *J. Chem. Phys.* **124**, 124302 (2006).
- <sup>23</sup>T. Morisato, S. N. Khanna, and Y. Kawazoe, *Phys. Rev. B* **72**, 014435 (2005).
- <sup>24</sup>E. Artacho, D. Sánchez-Portal, P. Ordejón, A. García, and J. M. Soler, *Phys. Status Solidi B* **215**, 809 (1999).
- <sup>25</sup>T. Oda, A. Pasquarello, and R. Car, *Phys. Rev. Lett.* **80**, 3622 (1998).
- <sup>26</sup>N. Troullier and J. L. Martins, *Phys. Rev. B* **43**, 1993 (1991).
- <sup>27</sup>J. P. Perdew, K. Burke, and M. Ernzerhof, *Phys. Rev. Lett.* **77**, 3865 (1996).
- <sup>28</sup>A. D. Becke, *Phys. Rev. A* **38**, 3098 (1988).